ECCOMAS Multibody Dynamics 2013
1-4 July, 2013, University of Zagreb, Croatia

Bifurcation Analysis of Self-excited Thermoacoustic Oscillations in Damper-equipped Combustion Chambers

Michael Baumann[1], Remco I. Leine[1], Nicolas Noiray[2], Bruno Schuermans[2]

[1] Institute of Mechanical Systems, Department of Mechanical and Process Engineering
ETH Zurich, 8092 Zürich, Switzerland, baumann@imes.mavt.ethz.ch
[2] Alstom Power
Brown Boveri Strasse, 5401 Baden, Switzerland, nicolas.noiray@power.alstom.com

Abstract

This paper presents the stability and bifurcation analysis of a nonlinear thermoacoustic model consisting of a combustion chamber coupled to a Helmholtz damper. Only the acoustic mode in the cavity of the combustion chamber to which the Helmholtz damper is tuned is considered. The Helmholtz damper includes a non-smooth damping term and can be seen as a tuned vibration absorber with a coupling on velocity level with non-vanishing gyroscopic terms.

Conditions for which self-sustained pressure oscillations are present in the coupled system are derived. Furthermore, the effects of nonlinearities on the stability properties of the system are investigated using standard techniques of multi-body dynamics. The bifurcation analysis shows a more rich dynamics than expected, considering that the investigated model describes the ideal case with perfectly tuned eigenfrequencies of the subsystems. The bifurcation branches of the occurring Hopf and fold bifurcations can be used to define a partition of the parameter space with different qualitative behaviour. The theoretical results are validated using numerical simulations.

Keywords: *bifurcation analysis, thermoacoustic coupling, tuned vibration absorber, Helmholtz damper*

1 Introduction

The mitigation of combustion instabilities is a challenging task in the development and improvement of gas turbines. This problem gains in importance due to progressively more stringent emission regulations. To meet this requirement the fuel/air mixing quality in the burners is constantly improved but this is often accompanied with an increase of pulsations due to thermoacoustic coupling. These oscillations result from constructive interaction between the flame and acoustic eigenmodes of the combustor and induce structural vibrations.

Thermoacoustic instabilities are induced by the coupling between the combustion dynamics, combustion noise and burner acoustics [8]. The combustion dynamics describes the flame response, i.e. the relation between fluctuations in the heat release rate and velocity perturbations. For a linear flame response this dynamics is commonly captured by the flame transfer function. Flames are essentially surfaces across which reactants are converted into products. The heat release can be perturbed by flame surface area fluctuations, which itself is sensitive to the acoustic velocity. The fluctuations in heat release rate induce unsteady gas expansions which generate acoustic pressure oscillations. This process is referred to as combustion noise. The pressure fluctuations propagate in the combustion chamber and get reflected and damped at the boundaries or at area discontinuities. The acoustic pressure and velocity oscillations can be sustained like in an organ-pipe and their coupling is described by the burner acoustics.

The investigation of combustion oscillations dates back to 1802 when Higgins [4] reported the phenomenon of the 'singing flame'. His experimental setup consisted of a gas flame which was placed in a tube being open at both ends. The flame excited a harmonic oscillation in the tube and, therefore, produced an audible sound. In 1878, Rayleigh [11, 12] stated his famous criterion

$$\int_T \int_V p'(\mathbf{x},t) q'(\mathbf{x},t) \mathrm{d}\mathbf{x}\mathrm{d}t > \int_T \int_V \Phi(\mathbf{x},t) \mathrm{d}\mathbf{x}\mathrm{d}t, \tag{1}$$

indicating the importance of the phase between the pressure oscillation and the unsteady heat release in encouraging the instability. The left-hand side of (1) captures the power transformed from the fluctuating heat release rate q' to the pressure oscillations p' during one oscillation cycle with period time T inside the control volume V. Thus, when the acoustic pressure and the heat release rate oscillations are in phase, total mechanical energy is added to the oscillation.

The dissipation in the acoustic field, which is not taken into account in the original criterion, is described by the wave energy dissipation Φ in the right-hand side of (1). If the energy addition overcomes the total energy dissipation, the acoustic energy in the combustor is increased, which leads to thermoacoustic instability of the combustion process.

There exist several passive and active means of control. Helmholtz dampers are commonly used to increase the acoustic dissipation (i.e. increase the term Φ in the Rayleigh Criterion (1)) and in turn decrease the amplitude of the pressure oscillations [1, 2]. Such acoustic resonators can be seen as tuned vibration absorbers commonly used to reduce mechanical vibrations. The ability of acoustic resonators to stabilize the system has to be evaluated prior to their implementation. In order to predict the damper performance, a greatly simplified theoretical model combining the combustion instability and the damper dynamics has been derived in [9]. This model has been extended to account for nonlinearities of the combustion chamber and the tuned acoustic vibration absorber.

Generally, linear analysis is used in the first acoustic design step. The eigenfrequency of the dampers are adjusted to the unstable mode, for which the acoustic absorption is maximized, and the stability of the equilibrium is determined by an eigenvalue analysis. However, the results of the present paper shows that it is of prime importance to consider the nonlinearities present in the system, since they significantly influence the system behaviour away from the equilibrium.

This paper presents the nonlinear stability and bifurcation analysis of a thermoacoustic model consisting of a combustion chamber with self-sustained pressure oscillation coupled to a Helmholtz damper. The thermoacoustic model, which is derived in Section 2, describes the acoustic pressure oscillation in the combustion chamber of one particular acoustic mode and the acoustic velocity oscillation in the neck of the Helmholtz damper. The ideal case of maximal acoustic absorption is considered, i.e. the eigenfrequency of the Helmholtz damper is adjusted to the unstable mode of the combustion chamber [3]. Section 3 presents the stability analysis including an eigenvalue analysis and the use of Lyapunov techniques. The bifurcation analysis has been conducted using the method of averaging (also called method of slowly changing phase and amplitude) and the results are compared to numerical simulations, which is shown in Section 4. A discussion of the results and concluding remarks are given in Section 5.

2 Model Derivation

The considered thermoacoustic model consists of a combustion chamber coupled to a Helmholtz damper (see Figure 1). The combustor dynamics and the dynamics of the Helmholz damper are derived separately and coupled afterwards via the acoustic velocity in the neck of the Helmholtz damper.

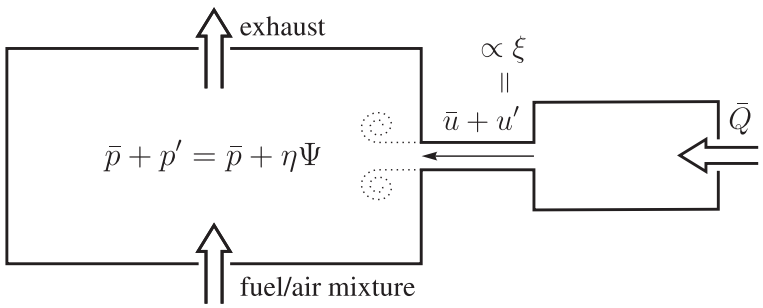

Figure 1. Thermoacoustic model consisting of a combustion chamber (left) coupled to a Helmholtz damper (right).

2.1 Dynamics of the Combustion Chamber

The variables pressure, velocity and heat release rate are decomposed into a mean part and a fluctuating part (also referred to as acoustic part). The mean part is assumed to be spatially constant and the fluctuating part is assumed to be small compared to the mean part. We assume no thermal conductivity to the surrounding, small Mach-numbers and viscous stresses to be negligible for low frequency acoustic perturbations. The acoustic pressure p' in the cavity of a combustion chamber with a fluctuating heat release rate q' is described by the forced acoustic wave equation [6]

$$\left(\frac{\partial^2}{\partial t^2} - \bar{c}^2\nabla^2\right) p' = (\gamma - 1)\frac{\partial}{\partial t} q', \tag{2}$$

where $\bar{c}$ is the average speed of sound and γ is the specific heat ratio. The boundary condition at the location of the Helmholtz damper imposes a acoustic impedance which couples the acoustic pressure to the acoustic velocity. The boundary condition away from the Helmholtz damper is either open (reflecting outlet) or closed (reflecting inlet). The open boundary is zeroing the pressure fluctuation (Dirichlet condition) and at the closed boundary the normal velocity vanishes (von-Neumann condition).

The acoustic pressure distribution is spanned on a complete orthonormal basis as $p'(\mathbf{x},t) = \sum_{i=0}^{\infty} \eta_i(t)\Psi_i(\mathbf{x})$, where the basis functions Ψ_i are defined by the acoustic eigenmodes of the system without acoustic sources. As an approximation, only the eigenmode with the largest growth rate is considered and all other eigenmodes are neglected, which corresponds to a Galerkin approach. The eigenfunction Ψ of the considered eigenmode is assumed to be real. This assumption is valid if the thermoacoustic coupling is weak and the surface where the damper with complex impedance is applied is small compared to the overall boundary. The interaction between the fluctuating heat release rate and the acoustic pressure as well as the acoustic flux across the control surface excluding the damper is captured by introducing a linear damping term κ_0. For negative values of κ_0, the constructive interaction is larger than the energy dissipation which leads to thermoacoustic instability of the undamped system (see Rayleigh Criterion (1)). The acoustic mode is therefore described by the linear damped oscillator

$$\frac{\mathrm{d}^2}{\mathrm{d}t^2}\eta + \kappa_0 \frac{\mathrm{d}}{\mathrm{d}t}\eta + \omega^2 \eta = 0, \tag{3}$$

where $\eta(t)$ is the participation factor of the Galerkin approach and ω is the eigenfrequency of the considered acoustic mode. The boundary condition at the location of the Helmholtz damper is described by the acoustic impedance which couples the acoustic pressure to the acoustic velocity perpendicular to the surrounding surface. Including additional nonlinear terms according to [10], we obtain a nonlinear forced oscillator as

$$\frac{\mathrm{d}^2}{\mathrm{d}t^2}\eta + \left(\kappa_0 + \kappa_1\eta^2 + \kappa_2\left(\frac{\mathrm{d}}{\mathrm{d}t}\eta\right)^2\right)\frac{\mathrm{d}}{\mathrm{d}t}\eta + \omega^2\eta = -\epsilon\chi\frac{\mathrm{d}}{\mathrm{d}t}u'. \tag{4}$$

The Van-der-Pol type terms with positive parameters κ_1 and κ_2 ensures boundedness of η for bounded acoustic velocities u'. The parameter $\chi > 0$ depends on fluid properties whereas $\epsilon > 0$ depends on the location of the Helmholtz damper w.r.t. the acoustic mode and therefore can be seen as the coupling efficiency of the two subsystems.

2.2 Dynamics of the Helmholtz Damper

A Helmholtz damper has a shape which is similar to a bottle. If the dimensions are small compared to the acoustic wavelength and the cross-sectional area of the bottle is much larger than the cross-sectional area of the neck, then the pressure perturbation inside the bottle can be assumed to be uniform. Therefore, the gas in the body acts as an acoustic spring whereas the gas in the neck acts as an acoustic mass. The damping of the resonator can be increased by a continuous volume flow $\bar{Q}$ injected into the bottle.

Assuming the flow to be uniform and frictionless, the dynamics of the acoustic velocity in the neck of the damper can be derived using the unsteady Bernoulli equation between a point at the entrance and a point at the exit of the neck as

$$\frac{\mathrm{d}^2}{\mathrm{d}t^2}u' + \zeta|\bar{u}+u'|\frac{\mathrm{d}}{\mathrm{d}t}u' + \omega_d^2 u' = \frac{\omega_d^2}{\chi}\frac{\mathrm{d}}{\mathrm{d}t}\eta, \tag{5}$$

where $\bar{u}$ is the mean flow due to the continuous volume flow $\bar{Q}$, ω_d is the eigenfrequency of the damper and $\zeta > 0$ is a damping efficiency. Depending on the sign of the velocity in the neck $u = \bar{u} + u'$, a jet on either side of the neck is formed. The pressure inside the quasi-stationary jet is assumed to be constant and equal to the external pressure, which is reasonable for small Mach-numbers. The Helmholtz damper can be seen as a vibration absorber with a non-smooth damping term.

2.3 Coupled Dynamics

The two subsystems described by (4) and (5) are coupled and the time as well as the states and parameters are normalized in order to write the model equations in a more manageable way. The time is normalised by the inverse natural frequency of the combustor as $\tau = \omega t$. Therefore, the time derivative becomes $\frac{\mathrm{d}}{\mathrm{d}t} = \omega\frac{\mathrm{d}}{\mathrm{d}\tau}$. We define $\dot{(\,)}$ as the derivative w.r.t. the dimensionless time τ. The acoustic velocity is normalized as $\xi = \frac{\chi}{\omega}u$ and new parameters are defined as $q = \frac{\kappa_0}{\omega}$,

$c_1 = \frac{\kappa_1}{\omega} > 0$, $c_2 = \omega\kappa_2 > 0$, $d = \frac{\zeta\bar{u}}{\omega} > 0$, $\delta = \frac{\zeta}{\chi} > 0$. Additionally, only the ideal case of a perfectly tuned vibration absorber is considered, i.e. $\omega = \omega_d$. Therefore, the coupled dynamics of (4) and (5) is obtained as

$$\ddot{\eta} + (q + c_1\eta^2 + c_2\dot{\eta}^2)\dot{\eta} + \eta = -\epsilon\dot{\xi}, \tag{6}$$

$$\ddot{\xi} + |d + \delta\xi|\dot{\xi} + \xi = \dot{\eta}. \tag{7}$$

From the viewpoint of multi-body dynamics, the dynamics of the acoustic pressure in the combustion chamber $\eta(t)$ is described by a mass-spring system with a Van der Pol-type damping (6) and the dynamics of normalized acoustic velocity in the neck of the Helmholtz damper $\xi(t)$ can be seen as a tuned vibration absorber with non-smooth damping (7). The coupling of the two systems is on velocity level with non-vanishing gyroscopic terms.

3 Stability Analysis

The coupled dynamics (6)-(7) has only one equilibrium, which is located at the origin. The stability of the equilibrium point is determined using Lyapunov's indirect method (see [5]). We introduce a new state vector $\mathbf{x} \in \mathbb{R}^4$ as $\mathbf{x} = \begin{pmatrix} x_1 & x_2 & x_3 & x_4 \end{pmatrix}^\mathsf{T} := \begin{pmatrix} \eta & \dot{\eta} & \xi & \dot{\xi} \end{pmatrix}^\mathsf{T}$. The linearization of the dynamics (6)-(7) in the new coordinate $\mathbf{x}$ is obtained as $\dot{\mathbf{x}} = \mathbf{A}\mathbf{x}$ with

$$\mathbf{A} = \begin{pmatrix} 0 & 1 & 0 & 0 \\ -1 & -q & 0 & -\epsilon \\ 0 & 0 & 0 & 1 \\ 0 & 1 & -1 & -d \end{pmatrix}. \tag{8}$$

The Hurwitz criterion gives us the following two conditions for which all eigenvalues of $\mathbf{A}$ have negative real part

$$\mu := \epsilon + dq > 0, \tag{9}$$

$$\nu := d + q > 0. \tag{10}$$

In the absence of thermoacoustic instability, i.e. $q > 0$, the conditions (9)-(10) are always fulfilled since $d > 0,\ \epsilon > 0$ and, thus, the equilibrium is asymptotically stable. The first condition (9) gives a lower bound for the coupling efficiency ϵ. Interestingly, if condition (9) is violated, then an increase of the linear damping d of the Helmholtz resonator does not stabilize the system. The second condition (10) states that the linear damping of the Helmholtz damper d must be larger than the linear growth rate q of the considered acoustic mode.

For small values of q, the eigenvalues appear as two complex conjugated pairs. According to conditions (9)-(10) we can define three regions:

Region I: $(\mu > 0 \wedge \nu > 0)$: both pairs of eigenvalues have negative real part and the equilibrium is stable,
Region II: $(\mu < 0)$: one pair of eigenvalues has negative real part, while the other pair has positive real part,
Region III: $(\mu > 0 \wedge \nu < 0)$: both pairs of eigenvalues have positive real part.

By continuously decreasing q we change from Region I to either Region II if $d^2 > \epsilon$ or to Region III if $d^2 < \epsilon$, i.e. depending on which condition is more restrictive. The latter transition is structurally unstable because it does not appear for an infinitesimal disturbance of the tuning of the Helmholtz damper. Therefore, we consider only transitions from Region I to Region II under the influence of the parameter μ, while assuming that the condition (10) is always fulfilled. At $\mu = 0$, one pair of complex conjugated eigenvalues cross the imaginary axis which gives rise to a Hopf bifurcation.

In order to determine the stability of the equilibrium it is sufficient to investigate the Jacobian matrix. Yet, depending on the nonlinearities, the attractivity property is only valid in a (possibly arbitrarily small) neighborhood of the equilibrium. The region of attraction, or at least a conservative estimate, can be found using Lyapunov's direct method (see [5]). Consider the Lyapunov function

$$V_1(\mathbf{x}) = \frac{1}{2}(\eta^2 + \dot{\eta}^2) + \frac{1}{2}\epsilon(\xi^2 + \dot{\xi}^2), \tag{11}$$

which is positive definite, since $\epsilon > 0$. The time derivative of (11), along solution curves of the coupled dynamics (6)-(7), is obtained as

$$\dot{V}_1(\mathbf{x}) = -(q + c_1\eta^2 + c_2\dot{\eta}^2)\dot{\eta}^2 - \epsilon\theta|d + \delta\xi|\dot{\xi}^2. \tag{12}$$

For $q > 0$ the derivative $\dot{V}_1$ is negative semi-definite, which proves stability of the equilibrium for $q > 0$ as we have seen in the eigenvalue analysis. The largest invariant set inside $\dot{V}_1 = 0$ is the equilibrium itself and, according to LaSalle's invariance principle [5], the equilibrium is globally asymptotically stable for $q > 0$. The Lyapunov function $V_1(\mathbf{x})$ is inconclusive for the case $q < 0$. We proceed by assuming a linear Helmholtz damper and consider the positive definite Lyapunov function and the corresponding time derivative given by

$$V_2(\mathbf{x}) = \frac{1}{2}\left((q\xi+\eta)^2 + (q\dot{\xi}+\dot{\eta})^2\right) + \frac{1}{2}\mu\left(\xi^2+\dot{\xi}^2\right), \tag{13}$$

$$\dot{V}_2(\mathbf{x}) = -(c_1\eta^2 + c_2\dot{\eta}^2)\left(\frac{q}{2}\dot{\xi}+\dot{\eta}\right)^2 - \left(\nu\mu - \left(\frac{q}{2}\right)^2(c_1\eta^2+c_2\dot{\eta}^2)\right)\dot{\xi}^2. \tag{14}$$

The derivative $\dot{V}_2$ is negative semidefinite for $\mu > 0$ and $\nu > 0$ inside the cylinder defined by $\frac{4\nu\mu}{q^2} \geq c_1\eta^2 + c_2\dot{\eta}^2$. Only local asymptotic stability can be shown using LaSalle's invariance principle. A global result is found using the additional assumption $c = c_1 = c_2$. Hereto, we add a positive semidefinite term to $V_2(\mathbf{x})$ and obtain

$$V_3(\mathbf{x}) = V_2(\mathbf{x}) + \frac{1}{4}\left(-\frac{qc}{\epsilon}\right)(\eta^2+\dot{\eta}^2)^2, \tag{15}$$

$$\dot{V}_3(\mathbf{x}) = -\nu\mu\dot{\xi}^2 - \frac{c}{\epsilon}(\mu - q\nu)(\eta^2+\dot{\eta}^2)\dot{\eta}^2 - \left(-\frac{qc^2}{\epsilon}\right)(\eta^2+\dot{\eta}^2)^2\dot{\eta}^2. \tag{16}$$

Using this Lyapunov function and the invariance principle, global asymptotic stability of the equilibrium of the coupled system (6)-(7) with $\delta = 0$ and $q < 0$ is proven for $\mu \geq 0$ and $\nu > 0$ under the assumption $c = c_1 = c_2$.

4 Bifurcation Analysis

The equilibrium of the system (6)-(7) is asymptotically stable for $\mu > 0$ and $\nu > 0$. At $\mu = 0$ one pair of eigenvalues cross the imaginary axis and the solutions remain bounded due to the Van-der-Pol type damping terms in the combustion dynamics (6). This gives rise to a supercritical Hopf bifurcation under the influence of the bifurcation parameter μ. The bifurcation can be approximated using common tools from nonlinear dynamics such as the center manifold reduction, the method of multiple scales [7] or the method of averaging [13, 14]. Due to the non-smooth damping terms, the most useful results can be obtained with the method of averaging, which is shown in the following.

The dynamics (6)-(7) is rewritten as

$$\ddot{\eta} - q\left(d\dot{\xi} - \dot{\eta}\right) + \eta = -\mu\dot{\xi} - (c_1\eta^2 + c_2\dot{\eta}^2)\dot{\eta}, \tag{17}$$

$$\ddot{\xi} + d\dot{\xi} - \dot{\eta} \qquad + \xi = \qquad -(|d+\delta\xi| - d)\dot{\xi}, \tag{18}$$

where $\mu = \epsilon + dq$ is chosen as the bifurcation parameter. The stationary solution of (17)-(18) for vanishing right-hand sides fulfills $\eta = d\xi$ and is given by

$$\eta = A\cos t + B\sin t, \tag{19}$$

$$\xi = C\cos t + D\sin t, \tag{20}$$

with constant coefficients $A = dC$ and $B = dD$.

Since the solutions η and ξ near the bifurcation are small, also the right-hand sides of (17)-(18) are small near the bifurcation, but do not exactly fulfill $\eta = d\xi$. According to the method of averaging, we assume that the solution of (17)-(18) can still be written in the form (19)-(20) for small μ, but with slowly time-varying coefficients $A(t)$, $B(t)$, $C(t)$ and $D(t)$. For time varying coefficients, the set of equations (19)-(20) define a variable transformation. Due to the slow time dependence, the terms which have a vanishing average over a period time $T = 2\pi$ are omitted. After several intermediate steps, the transformed dynamics is obtained as

$$\dot{A} = \frac{1}{2}(dq-\mu)C - \frac{1}{2}\left(q + \frac{c_1+3c_2}{4}(A^2+B^2)\right)A, \tag{21}$$

$$\dot{B} = \frac{1}{2}(dq-\mu)D - \frac{1}{2}\left(q + \frac{c_1+3c_2}{4}(A^2+B^2)\right)B, \tag{22}$$

$$\dot{C} = -\frac{1}{2}d(1+g(a))C + \frac{1}{2}A, \tag{23}$$

$$\dot{D} = -\frac{1}{2}d(1+g(a))D + \frac{1}{2}B, \tag{24}$$

where

$$g(a) = \begin{cases} \frac{2}{\pi}\left(\frac{\sqrt{a^2-1}(1+2a^2)}{3a^2} - \arccos\frac{1}{|a|}\right) & \text{for } |a| > 1, \\ 0 & \text{for } |a| \leq 1, \end{cases} \tag{25}$$

$$a = \frac{\delta}{d}\sqrt{C^2+D^2}. \tag{26}$$

According to the transformation (19)-(20), the amplitudes of oscillation in the original coordinates ξ and η are given by

$$r_\xi = \sqrt{C^2+D^2}, \tag{27}$$

$$r_\eta = \sqrt{A^2+B^2}. \tag{28}$$

The dynamics (21)-(24) has an equilibrium at the origin, which is stable for $\mu \geq 0$ and unstable otherwise, which corresponds to results obtained from the eigenvalue analysis. The nontrivial equilibria of (21)-(24) are given by the implicit equations

$$r_\xi^2 = -\frac{4(\mu + dqg(a))}{d^3(c_1+3c_2)(1+g(a))^3}, \tag{29}$$

$$r_\eta^2 = -\frac{4(\mu + dqg(a))}{d(c_1+3c_2)(1+g(a))} = d^2(1+g(a))^2 r_\xi^2. \tag{30}$$

For a linear Helmholtz damper, i.e. $\delta = 0$, we have $a = 0$ and $g(a) = 0$ according to (25)-(26) and the nontrivial equilibria are obtained as

$$r_\xi^2 = -\frac{4\mu}{d^3(c_1+3c_2)}, \tag{31}$$

$$r_\eta^2 = -\frac{4\mu}{d(c_1+3c_2)}. \tag{32}$$

The equilibria (31)-(32) exist only for $\mu < 0$. One of the four eigenvalues is at zero and the others are in the left open half complex plane for $\mu < 0$. The zero eigenvalue expresses the 'freedom of phase' because the system is autonomous. We note that for a linear Helmholtz damper a supercritical Hopf bifurcation occurs. The stable periodic solution branching off at $\mu = 0$ corresponds to a harmonic oscillation in the original coordinates η and ξ with unit frequency and an amplitude given by (31)-(32).

In order to find the periodic solutions for a nonlinear Helmholtz damper, we rewrite (29) with (26) and (27) as

$$a^2 - k_1^2 \frac{k_2 + g(a)}{(1+g(a))^3} = 0, \tag{33}$$

where

$$k_1 = \frac{2\delta}{d^2}\sqrt{-\frac{q}{(c_1+3c_2)}}, \tag{34}$$

$$k_2 = \frac{\mu}{dq}. \tag{35}$$

We consider only negative q, because for $q > 0$ no periodic solutions exist as shown in Section 3. Therefore, k_1 is always positive and k_2 is positive for negative μ and vice versa. The roots of (33) correspond to harmonic oscillations of the states η and ξ with a unit frequency and an amplitude given by

$$r_\xi = \frac{d}{\delta}a, \tag{36}$$

$$r_\eta = \frac{d^2}{\delta}(1+g(a))a. \tag{37}$$

Figure 2 shows the scaled amplitude of oscillation of ξ as a function of the new bifurcation parameter k_2 for different values of k_1. The black lines correspond to stable periodic solutions, whereas the grey lines correspond to unstable periodic solutions. According to (35), the equilibrium is unstable for $k_2 > 0$ and stable otherwise. The parameter k_1,

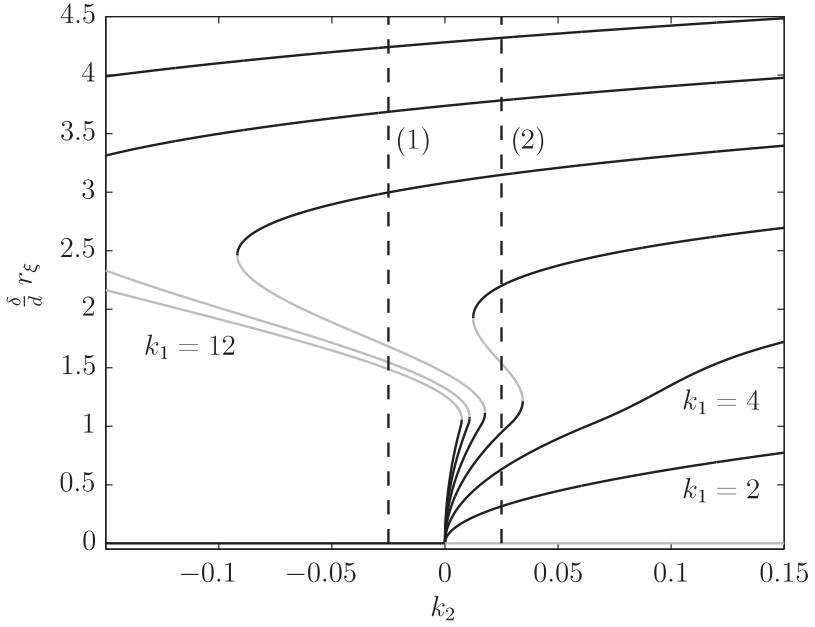

Figure 2. Stable (black) and unstable (grey) periodic solutions for different values of k_1 and k_2. Depicted is the amplitude of oscillation of ξ, scaled by the factor $\frac{\delta}{d}$.

defined by (34), captures the linear and nonlinear damping in the system and, most importantly, it is proportional to δ. Therefore, k_1 captures the nonlinearity of the Helmholtz damper. For a weakly nonlinear Helmholtz damper, i.e. $k_1 < 5.2$, the system experiences only a Hopf bifurcation under the influence of the parameter k_2. For $k_1 > 5.2$ two additional fold bifurcations occur and we have coexistence of stable limit sets. Keeping k_1 fixed, e.g. at $k_1 = 6$, and slowly sweeping k_2 up and down, the solution follows the stable branches and 'jump' at the fold bifurcations from one periodic solution to the other, which leads to a hysteresis effect. For $k_1 > 6.2$ the 'elbow' in Figure 2 even reaches inside the region where $k_2 < 0$ and the equilibrium is only locally asymptotically stable.

At Section (1) (left dotted line in Figure 2), there exist a stable equilibrium without coexisting periodic solutions for small k_1, which is depicted in Figure 3 labelled with (1a). For a highly nonlinear Helmholtz damper there are additionally a stable and an unstable periodic solution, which is shown in Figure 2 labelled with (1b). At Section (2) (right dotted line in Figure 2), the equilibrium is unstable and it is either surrounded by one stable periodic solution (k_1 small), depicted in Figure 3 labelled with (2a), or it coexists with three periodic solutions with alternating stability (k_1 large), which is shown in Figure 3 labelled with (2b).

The location of the bifurcations in the k_1-k_2-plane is depicted in Figure 5. The dashed line shows the location of the supercritical Hopf bifurcation and the solid lines show at which location the fold bifurcations occur. The two fold bifurcations meet at $(k_2,\, k_1) = (0.051,\, 5.2)$. At this point, the fold bifurcations cancel each other out and we have a cusp catastrophe, which is a bifurcation of codimension 2. One fold bifurcation tends to infinity for $k_2 \to 0^+$. This can be seen be expanding (33) in a Taylor series around $a = 1$ and omitting terms of higher order than $\mathcal{O}\left((a-1)^2\right)$, which yields $a^2 - k_1^2 k_2 = 0$. The escaping fold bifurcation asymptotically approaches $k_1 = \sqrt{\frac{1}{k_2}}$ in the k_1-k_2-plane.

As it shown in Figure 5, the parameter space is partitioned into four regions (1a), (1b), (2a) and (2b). The periodic solutions occurring in each region are depicted in Figure 3. For a weakly nonlinear Helmholtz resonator, i.e. $k_1 < 5.2$, we have only a Hopf bifurcation and no fold bifurcations. The stable equilibrium has possibly coexisting periodic solutions if $k_1 > 6.2$.

The limit sets of the original coupled dynamics (6)-(7) are computed using computer simulations for four different parameter sets and they are depicted in Figure 4 in the scaled ξ-$\dot{\xi}$-plane. The stable (black) and unstable (grey) limit sets are drawn with solid lines and the dotted lines show the limit sets obtained using the method of averaging. The system parameters $q = -0.1$, $d = 0.3$, $c_1 = 0.001$, and $c_2 = 0$ are the same in all four cases and the parameters δ and ϵ are chosen such that the parameters k_1 and k_2 are $k_1 = 5$, $k_2 = -0.02$ (corresponding to case (1a)) for the top left plot, $k_1 = 8$, $k_2 = -0.02$ (corresponding to case (1b)) for the top right plot, $k_1 = 8$, $k_2 = 0.04$ (corresponding to case (2a))

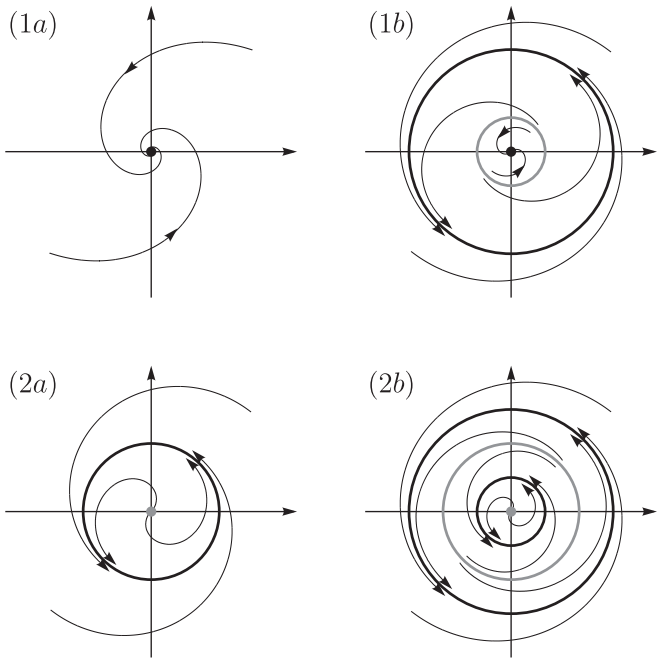

Figure 3. The stable equilibrium either has no coexisting periodic solutions (top left) or it is surrounded by a stable and an unstable periodic solution (top right). The unstable equilibrium is surrounded by either one stable periodic solution (bottom left) or it coexists with three periodic solutions with alternating stability (bottom right).

for the bottom left plot and $k_1 = 8$, $k_2 = 0.01$ (corresponding to case (2b)) for the bottom right plot in Figure 4. The comparison shows that the averaging results are valid as long as the amplitudes are slowly changing.

5 Conclusions

The coupled model of a combustion chamber with a perfectly tuned Helmholtz damper is derived. Only one acoustic mode in the cavity of the combustion chamber is considered. The dynamics of the participation factor of the Galerkin approach is described by a mass-spring system. The linear damping is positive in the presence of destructive interaction between the flame and the considered acoustic eigenmode. The nonlinear damping terms ensure boundedness of the solutions. The Helmholtz damper can be seen as a tuned acoustic vibration absorber with non-smooth damping. The coupling of the two subsystems include non-vanishing gyroscopic terms which makes it difficult to find a simple mechanical analogon.

In the absence of thermoacoustic instability the quiescent state is globally asymptotically stable. In the more interesting case of thermoacoustic instability the use of a Helmholtz damper is necessary. The linear damping of the Helmholtz damper is assumed to be sufficiently large and the coupling efficiency and the nonlinearity of the Helmholtz damper are varied. For a linear or weakly nonlinear Helmholtz damper, asymptotic stability can still be achieved. Decreasing the coupling efficiency a supercritical Hopf bifurcation occurs and the stable periodic solution branching off at this point represent a self-sustained oscillation. The acoustic pressure in the combustion chamber and the acoustic velocity in the neck of the Helmholtz damper oscillate at the same frequency and with a vanishing phase shift. In contrast to this, the bifurcation analysis for a highly nonlinear Helmholtz damper shows a more rich dynamics than expected, considering that the investigated model describes the ideal case with perfectly tuned eigenfrequencies of the subsystems. Increasing the parameter capturing the nonlinearity of the Helmholtz damper additional fold bifurcations can occur which leads to additional periodic solutions. An important result is that the stable equilibrium will eventually become only locally attractive due to coexisting limit cycles. Additionally, the presence of coexisting stable limit sets explains the hysteresis-effect observed in experiments where a system parameter is changed quasi-stationary.

The six system parameters have been reduced to only two relevant parameters. The bifurcation branches of the Hopf bifurcation and the fold bifurcations as a function of these new parameters define a partition of the parameter space with four regions of which every region has a different number of limit sets. A cusp catastrophe happens where the two branches of the fold bifurcations meet.

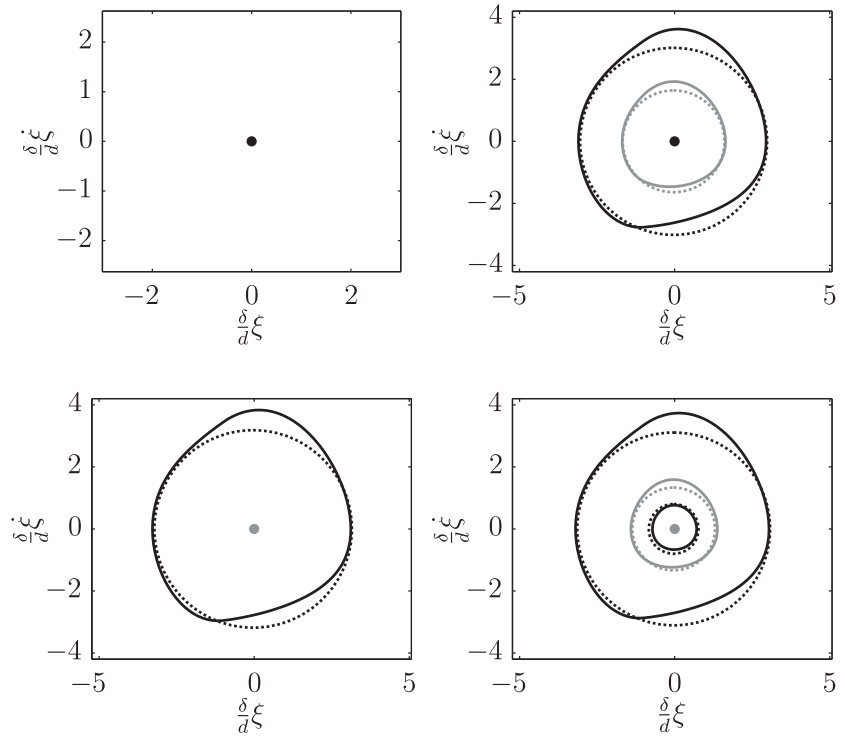

Figure 4. Stable (black) and unstable (grey) limit sets in the scaled ξ-$\dot{\xi}$-plane obtained using simulations of the full non-smooth coupled system (solid) and using the method of averaging (dotted) for different values of k_1 and k_2: top left: $k_1 = 5$, $k_2 = -0.02$ (case (1a)); top right: $k_1 = 8$, $k_2 = -0.02$ (case (1b)); bottom left: $k_1 = 8$, $k_2 = 0.04$ (case (2a)); bottom right: $k_1 = 8$, $k_2 = 0.01$ (case (2b)).

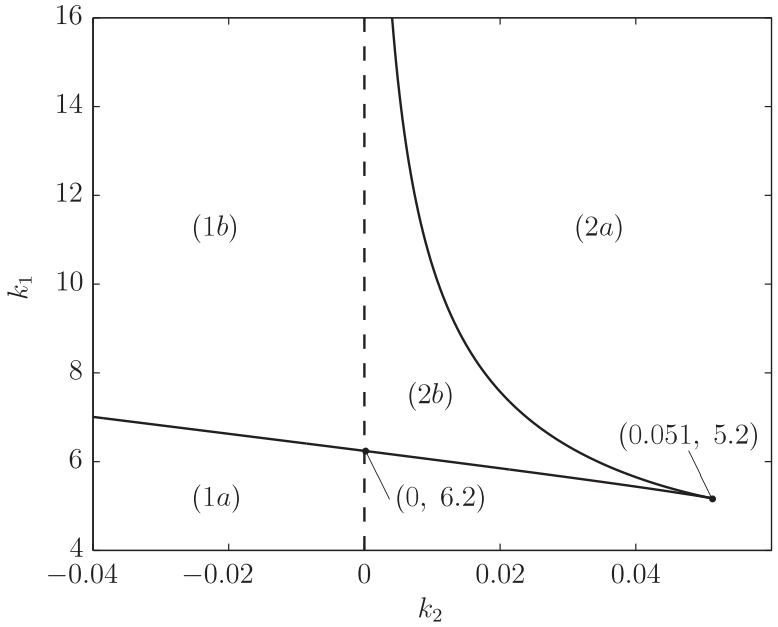

Figure 5. Hopf bifurcation (dashed) and fold bifurcations (solid) in the k_1-k_2-plane. A cusp catastrophe occurs at $(k_2,\, k_1) = (0.051,\, 5.2)$.

Acknowledgement

This research is supported by the Swiss National Science Foundation (SNF 200021-144307).

References

[1] V. Bellucci, B. Schuermans, D. Nowak, P. Flohr and C. O. Paschereit. Thermoacoustic modeling of a gas turbine combustor equipped with acoustic dampers. *Journal of Turbomachinery - Transactions of the ASME*, 127(2):372-379, 2005.

[2] I. D. J. Dupère and A. O. Dowling. The use of Helmholtz resonators in a practical combustor. *Journal of Engineering for Gas Turbines and Power - Transactions of the ASME*, 127(2):268-275, 2005.

[3] F. J. Fahy and C. Schofield. A note on the interaction between a Helmholtz resonator and an acoustic mode of an enclosure. *Journal of Sound and Vibration*, 72(3):365-378, 1980.

[4] B. Higgins. Letter from Dr. Higgins to Mr. Nicholson. *Journal of Natural Philosophy, Chemistry, and the Arts*, I:130-131, 1802.

[5] H. K. Khalil. *Nonlinear Systems*, 3rd ed. Prentice Hall, Upper Saddle River, 2002.

[6] P. M. Morse and K. U. Ingard. *Theoretical Acoustics*. Princeton University Press, Princeton, 1968.

[7] A. H. Nayfeh. *The Method of Normal Forms*, vol. 2. Wiley-VCH Verlag, Weinheim, 2011.

[8] N. Noiray, D. Durox, T. Schuller and S. Candel. A unified framework for nonlinear combustion instability analysis based on the flame describing function. *Journal of Fluid Mechanics*, 615:139-167, 2008.

[9] N. Noiray and B. Schuermans. Theoretical and experimental investigations on damper performance for suppresion of thermoacoustic oscillations. *Journal of Sound and Vibration*, 331(12):2753-2763, 2012.

[10] N. Noiray and B. Schuermans. Deterministic quantities characterizing noise driven Hopf bifurcations in gas turbine combustors. *International Journal of Non-Linear Mechanics*, 50():152-163, 2013.

[11] J. W. S. Rayleigh. The explanation of certain acoustic phenomena. *Nature*, 18(455):319-321, 1878.

[12] J. W. S. Rayleigh. *The Theory of Sound*. Macmillan, London, 1894.

[13] F. Verhulst. *Methods and Applications of Singular Perturbations: Boundary Layers and Multiple Timescale Dynamics*. Springer, New York, 2005.

[14] F. Verhulst. *Nonlinear Differential Equations and Dynamical Systems*, vol. 3. Springer, Berlin, 2006.